

In situ polymerization preparation and characterization of $\text{Li}_4\text{Ti}_5\text{O}_{12}$ -polyaniline anode material

HE Ze-qiang(何则强)^{1,2}, XIONG Li-zhi(熊利芝)^{1,2}, CHEN Shang(陈 上)¹,
WU Xian-ming(吴显明)¹, LIU Wen-ping(刘文萍)¹, HUANG Ke-long(黄可龙)²

1. College of Biology and Environmental Sciences, Jishou University, Jishou 416000, China;

2. School of Chemistry and Chemical Engineering, Central South University, Changsha 410083, China

Received 6 July 2009; accepted 30 December 2009

Abstract: $\text{Li}_4\text{Ti}_5\text{O}_{12}$ powders were prepared by so-gel method using tetrabutyl titanate, lithium acetate and absolute alcohol as starting materials. $\text{Li}_4\text{Ti}_5\text{O}_{12}$ -polyaniline ($\text{Li}_4\text{Ti}_5\text{O}_{12}$ -PAN) composite was prepared by in situ polymerization method using aniline, ammonium persulfate and hydrochloric acid as starting materials. $\text{Li}_4\text{Ti}_5\text{O}_{12}$ -PAN composite was characterized by X-ray diffractometry (XRD), infrared spectrum (IR) combined with electrochemical tests. The results show that the electrical conductivity is enhanced obviously due to the introduction of PAN to $\text{Li}_4\text{Ti}_5\text{O}_{12}$. $\text{Li}_4\text{Ti}_5\text{O}_{12}$ -PAN composite exhibits better high-rate capability and cyclability than $\text{Li}_4\text{Ti}_5\text{O}_{12}$. The composite can deliver a specific capacity of 191.3 and 148.9 mA·h/g, only 0.13% and 0.61% of the capacity is lost after being discharged 80 times at 0.1C and 2.0C, respectively.

Key words: $\text{Li}_4\text{Ti}_5\text{O}_{12}$; polyaniline; in situ polymerization method; lithium ion batteries

1 Introduction

Due to its good structural stability (zero-strain insertion material)[1–2] and satisfactory safety in the charge–discharge process, $\text{Li}_4\text{Ti}_5\text{O}_{12}$ is thought as a good anode material for asymmetrical mixed battery and lithium ion batteries with high power. However, lower lithium-ion conductivity and low electronic conductivity of $\text{Li}_4\text{Ti}_5\text{O}_{12}$ lead to poor rate capability[3–6]. To overcome this shortcoming, many methods have been developed, such as sol-gel, doping and nanotechnologies [1–2, 7]. The results showed that an electronically conductive agent such as Ag was very useful to improve the high-rate performance of $\text{Li}_4\text{Ti}_5\text{O}_{12}$ [8]. However, the high cost of Ag urges us to develop new conducting additive. To find a cheaper conducting additive is one of the keys for the practical application of $\text{Li}_4\text{Ti}_5\text{O}_{12}$. Carbon is a good conducting material and used widely in lithium ion batteries. If $\text{Li}_4\text{Ti}_5\text{O}_{12}$ is coated with carbon on its surface, the good conductivity of carbon can make up for the poor conductivity of $\text{Li}_4\text{Ti}_5\text{O}_{12}$ and improve its electrochemical properties. GUERFI et al[9–10]

investigated the effects of carbon black, high-surface-area carbon, graphite and carbonized polymer on the structure, morphology and electrochemical properties. According to their results, the carbon has three roles as follows: 1) As reducing agent, the carbon improves the reaction in the bulk powders and increases lithium diffusion in the particles to enhance complete transformation; 2) The carbon additive helps to reduce the particle size and produce an agglomerate of small particles in a chain-like structure; 3) The carbon increases the inter-particle contact and disturbs the undesirable particle growth. Hence, it is possible to obtain $\text{Li}_4\text{Ti}_5\text{O}_{12}$ material with good performance by using different types of carbons. HE et al[11] have reported $\text{Li}_4\text{Ti}_5\text{O}_{12}$ -C composite synthesized by sol-gel method to improve the electrochemical properties, especially the high rate cycling performance of $\text{Li}_4\text{Ti}_5\text{O}_{12}$.

Recently, the conducting polymer has been studied as an additive to improve the performances of cathode and anode materials in lithium ion batteries[12–14]. The conducting polymer composites exhibit good charge-discharge properties, indicating clearly that the conducting polymer can work as a conducting matrix for

Foundation item: Project(20376086) supported by the National Natural Science Foundation of China; Project(2005037700) supported by Postdoctoral Science Foundation of China; Project(07JJ3014) supported by Hunan Provincial Natural Science Foundation of China; Project(07A058) supported by Scientific Research Fund of Hunan Provincial Education Department; Project(2004107) supported by Postdoctoral Science Foundation of Central South University, China

Corresponding author: HE Ze-qiang; Tel: +86-743-8563911; E-mail: csuhzq@163.com

the particles of electrode. HE et al[15] have reported the SnO_2 -polyaniline(SnO_2 -PAN) composite prepared by microemulsion polymerization method. The results show that conductive PAN particles help to improve the contact of between Sn particles in the electrode reaction process and enhance the cycling performance of nano- SnO_2 .

However, using polyaniline powder as an additive for a $\text{Li}_4\text{Ti}_5\text{O}_{12}$ anode material in lithium-ion batteries has not been explored. In this work, $\text{Li}_4\text{Ti}_5\text{O}_{12}$ -polyaniline composite was synthesized using the in situ polymerisation method. The possibility of using $\text{Li}_4\text{Ti}_5\text{O}_{12}$ -polyaniline composite as an anode material for lithium ion batteries was examined.

2 Experimental

6.151 g lithium acetate was solved in a certain quantity of ethanol absolute and 10 mL tetrabutyl titanate was added according to the molar ratio of Li to Ti of 4:5 with stirring for 30 min to get a precursor solution of $\text{Li}_4\text{Ti}_5\text{O}_{12}$. This solution was added with several droplets of deionized water and kept at 100 °C for 4 h to obtain a white or light yellow dry gel. The dry gel was calcinated at 800 °C for 20 h in muffer furnace and milled to get $\text{Li}_4\text{Ti}_5\text{O}_{12}$ powders.

0.01 mol aniline and ammonium persulfate were solved in 25 mL 1 mol/L HCl. When the ammonium persulfate solution was added to aniline solution, time was recorded. After 3 min, $\text{Li}_4\text{Ti}_5\text{O}_{12}$ powders were added to this system according to $w(\text{PAN}):w(\text{Li}_4\text{Ti}_5\text{O}_{12})=1:19$ and the reaction was kept at 30 °C for 18 h. After filtering, the product was washed with 0.2 mol/L HCl, 50 mL acetone and 0.2 mol/L HCl, respectively, and immersed in 50 mL 1 mol/L HCl (in which 0.01 mol aniline solved) for 1.5 h. Then the residue was washed with 0.2 mol/L HCl and acetone three times and dried at 60 °C to constant mass in vacuum to get $\text{Li}_4\text{Ti}_5\text{O}_{12}$ -PAN composite.

Phase identification studies of the samples were carried out by an X-ray diffractometer (XRD; Rigaku D/MAX-gA) with $\text{Cu K}\alpha$ radiation. The infrared (IR) spectra of the samples were conducted on a Fourier transform infrared spectrometer (Nicolet).

A slurry containing 80% (mass fraction) $\text{Li}_4\text{Ti}_5\text{O}_{12}$ -PAN composite, 10% acetylene black and 10% PVDF (polyvinylidene fluoride) was made using *N*-methylpyrrolidinone (NMP) as the solvent. Electrodes with an area of 1 cm^2 for the measurements of electrochemical characterization were prepared by coating slurries (about 100 μm in thickness) on copper foils followed by drying in vacuum at 60 °C for 12 h. Electrochemical tests were conducted using a conventional coin-type cell, employing lithium foil as a counter electrode and utilizing 1.0 mol/L LiPF_6 in

ethylene carbonate/dimethyl carbonate (EC/DMC) (with volume ratio of EC to DMC of 1:1) as the electrolyte. The assembly was carried out in an Ar-filled glove box. The electrochemical analyses were carried out with an electrochemical analysis system.

3 Results and discussion

Fig.1 shows the XRD patterns of PAN, $\text{Li}_4\text{Ti}_5\text{O}_{12}$ and $\text{Li}_4\text{Ti}_5\text{O}_{12}$ -PAN. All XRD peaks in Fig.1(a) are in the range of $2\theta=10^\circ\text{--}30^\circ$, indicating that the prepared PAN has a pseudo-orthorhombic crystal structure, in which single-chain of polymers and Cl^- is in a way of close packing[16]. XRD peaks in Fig.1(b) agree well with those of the standard JCPDS card No.490207, suggesting that the synthesized sample is spinel $\text{Li}_4\text{Ti}_5\text{O}_{12}$. $\text{Li}_4\text{Ti}_5\text{O}_{12}$ shares a face centered cubic structure with a space group of $Fd\bar{3}m$ ($a=8.36$ Å), in which Li^+ is in 8a-site of tetrahedron, Ti^{4+} is in 16d-site of octahedron (the molar ratio of Li to Ti is 4:5), while O^{2-} is in sites of 32e [17–18]. There is no peak between $2\theta=10^\circ\text{--}30^\circ$ in Fig.1(c), which indicates that PAN in $\text{Li}_4\text{Ti}_5\text{O}_{12}$ -PAN composite is in amorphous form and the exist of $\text{Li}_4\text{Ti}_5\text{O}_{12}$ affects the XRD pattern of PAN significantly. It may be caused by the deposition of PAN on the surface of $\text{Li}_4\text{Ti}_5\text{O}_{12}$ particle, which prevents the crystallization of PAN and is very similar to the result of Fusalba[19]. They found that the exist of MoS_3 in PAN/ MoS_3 composite reduces the crystallization of PAN.

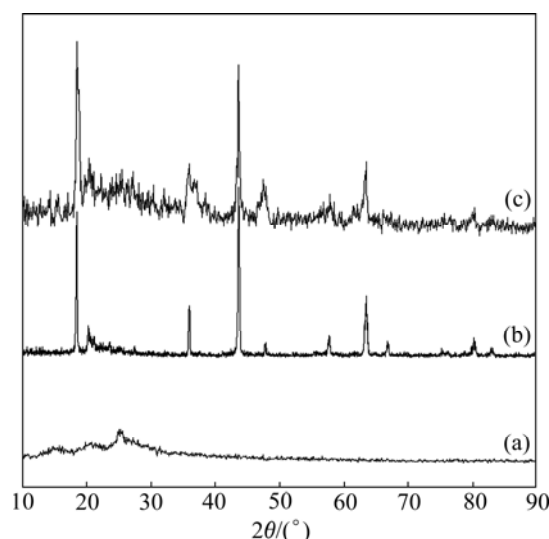


Fig.1 XRD patterns of PAN(a), $\text{Li}_4\text{Ti}_5\text{O}_{12}$ (b) and $\text{Li}_4\text{Ti}_5\text{O}_{12}$ -PAN (c)

Fig.2 presents the IR spectra of PAN, $\text{Li}_4\text{Ti}_5\text{O}_{12}$ and $\text{Li}_4\text{Ti}_5\text{O}_{12}$ -PAN. In the IR spectrum (Fig.2(a)) of PAN, four strong characteristic absorption bands appear at 819, 1 131, 1 299 and 3 454 cm^{-1} , are assigned to C—H out-of-plane bending vibration, $\text{N}=\text{Ar}=\text{N}$ mode of

vibration, C—N stretching vibration and N—H stretching vibration of two substituted benzenes, respectively. The absorption bands at 1 497 and 1 581 cm^{-1} are attributed to skeletal vibration of N—Ar—N and N=Ar=N[20]. Fig.2(b) shows the IR spectrum of $\text{Li}_4\text{Ti}_5\text{O}_{12}$, and the absorption bands at 676.8 and 457.0 cm^{-1} present the symmetrical stretching vibration and asymmetrical stretching vibration of Ti—O[21], respectively. In the IR spectrum of $\text{Li}_4\text{Ti}_5\text{O}_{12}$ -PAN composite (Fig.2(c)), except for the characteristic absorption bands assigned to PAN, there appear peaks at 676.8 and 457.0 cm^{-1} assigned to Ti-O stretching vibration too, indicating that $\text{Li}_4\text{Ti}_5\text{O}_{12}$ -PAN composite shows the common characteristics of PAN and $\text{Li}_4\text{Ti}_5\text{O}_{12}$ and is the complex of PAN and $\text{Li}_4\text{Ti}_5\text{O}_{12}$.

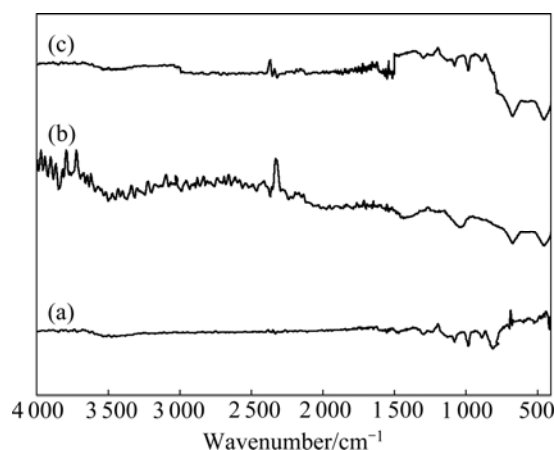


Fig.2 IR spectra of of PAN(a), $\text{Li}_4\text{Ti}_5\text{O}_{12}$ (b) and $\text{Li}_4\text{Ti}_5\text{O}_{12}$ -PAN (c)

Fig.3 shows the first discharge curves of $\text{Li}_4\text{Ti}_5\text{O}_{12}$ -PAN composite and $\text{Li}_4\text{Ti}_5\text{O}_{12}$. On the discharge curves of both materials, a long plateau at 1.60 V appears, which corresponds to the normal reversible change of active material $\text{Li}_4\text{Ti}_5\text{O}_{12}$ [8, 22–23], namely, the active material converts from $\text{Li}_4\text{Ti}_5\text{O}_{12}$ to $\text{Li}_7\text{Ti}_5\text{O}_{12}$ with the reduction of Ti^{4+} to Ti^{3+} of 1 mol. Meanwhile, a short plateau at 0.6–0.7 V appears, which may be associated with the further reduction of the remaining Ti^{4+} in $\text{Li}_4\text{Ti}_5\text{O}_{12}$ to Ti^{3+} , suggesting a multi-step restore of Li^+ during the discharge period of $\text{Li}_4\text{Ti}_5\text{O}_{12}$ [24]. The first discharge capacity of $\text{Li}_4\text{Ti}_5\text{O}_{12}$ -PAN is 191.3 $\text{mA}\cdot\text{h/g}$, slightly less than that of $\text{Li}_4\text{Ti}_5\text{O}_{12}$. However, the discharge capacities of two materials are to some extent higher than the theoretical specific capacity of the spinel $\text{Li}_4\text{Ti}_5\text{O}_{12}$, 175 $\text{mA}\cdot\text{h/g}$ [25]. The extra capacity must be associated with the second platform at 0.6–0.7 V, suggesting the further reduction of the remaining Ti^{4+} .

Fig.4 shows the first discharge curves of $\text{Li}_4\text{Ti}_5\text{O}_{12}$ -PAN at various current rates. From Fig.4, three effects can be found as follows: 1) Cell voltage decreases with the increase of discharge current. It is 1.60 V at

0.1C and drops to about 1.35 V at 2.0C. 2) The discharge capacity of $\text{Li}_4\text{Ti}_5\text{O}_{12}$ -PAN exhibits a tendency to decrease with the increase of discharge current rate. It is 191.3 $\text{mA}\cdot\text{h/g}$ at 0.1C and decreases to about 148.9 $\text{mA}\cdot\text{h/g}$ at 2.0C. 3) With the discharge current rate increasing, the discharge capacity increases in 0.6–0.7 V, which agrees well with the results of $\text{Li}_4\text{Ti}_5\text{O}_{12}/\text{Ag}$ composite[10, 24].

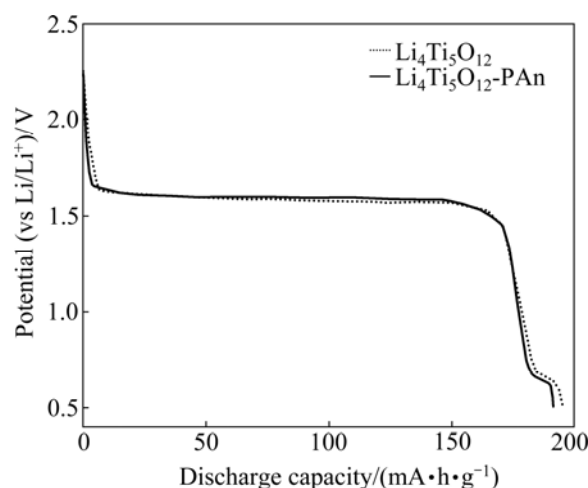


Fig.3 First discharge curves of $\text{Li}_4\text{Ti}_5\text{O}_{12}$ -PAN and $\text{Li}_4\text{Ti}_5\text{O}_{12}$ at 0.1C (2.5–0.5 V)

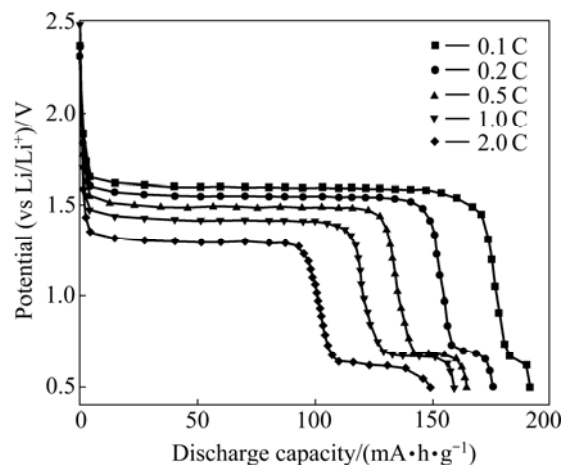


Fig.4 First discharge curves of $\text{Li}_4\text{Ti}_5\text{O}_{12}$ -PAN at various current rates (2.5–0.5 V)

The cyclabilities of $\text{Li}_4\text{Ti}_5\text{O}_{12}$ -PAN composite at various current rates were conducted as shown in Fig.5. With the current rate increasing, the discharge capacity decreases. After cycling 80 times, the discharge capacity at 0.1C decreases from 191.3 $\text{mA}\cdot\text{h/g}$ to 172.0 $\text{mA}\cdot\text{h/g}$, and the capacity loss per cycle is 0.13%; while the discharge capacity at 2.0C decreases from 148.9 $\text{mA}\cdot\text{h/g}$ to 76.2 $\text{mA}\cdot\text{h/g}$, the capacity loss per cycle is 0.61%. This result shows that small current rate reduces the cell polarization; therefore, the capacity loss decreases and the cycling performance of $\text{Li}_4\text{Ti}_5\text{O}_{12}$ -PAN composite is improved.

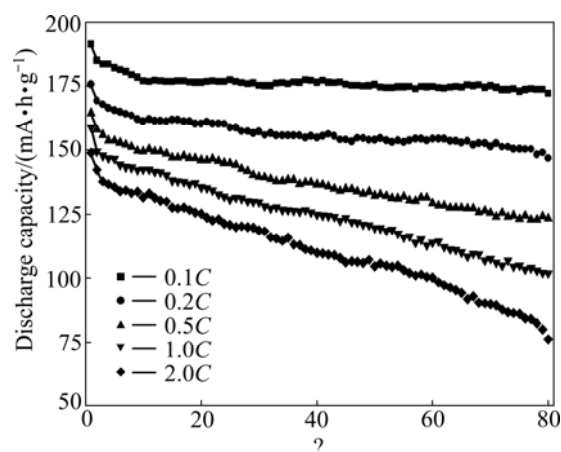


Fig.5 Cyclability of $\text{Li}_4\text{Ti}_5\text{O}_{12}$ -PAN at various current rates (2.5–0.5 V)

Comparison of cycling performance for $\text{Li}_4\text{Ti}_5\text{O}_{12}$ -PAN and $\text{Li}_4\text{Ti}_5\text{O}_{12}$ anode materials is summarized in Table 1. It is obvious that the discharge capacity of $\text{Li}_4\text{Ti}_5\text{O}_{12}$ -PAN composite is slightly less than that of $\text{Li}_4\text{Ti}_5\text{O}_{12}$ because the ratio of active material $\text{Li}_4\text{Ti}_5\text{O}_{12}$ decreases when PAN is added to $\text{Li}_4\text{Ti}_5\text{O}_{12}$ to form composite. With the discharge current rate increasing, the cell polarization increases and the discharge capacities of two materials decrease. The capacity loss per cycle after cycling 10 times for $\text{Li}_4\text{Ti}_5\text{O}_{12}$ -PAN composite is slightly lower than that of $\text{Li}_4\text{Ti}_5\text{O}_{12}$. When discharged at 2.0C, the reversible capacity of $\text{Li}_4\text{Ti}_5\text{O}_{12}$ is 125.9 mA·h/g and the capacity loss per cycle is 1.57% after cycling 10 times; under the same conditions, the reversible capacity of $\text{Li}_4\text{Ti}_5\text{O}_{12}$ -PAN is more than 131.6 mA·h/g and the capacity loss per cycle is only 1.16%. Similar to the $\text{Li}_4\text{Ti}_5\text{O}_{12}$ /Ag composite[10,24], since the electronic conductivity of the pristine $\text{Li}_4\text{Ti}_5\text{O}_{12}$ is very low, the conductive PAN additive significantly enhances the surface intercalation reaction and reduces the cell polarization; therefore, the rate performance of the composite is improved.

In order to compare the conductivity of $\text{Li}_4\text{Ti}_5\text{O}_{12}$ -PAN and $\text{Li}_4\text{Ti}_5\text{O}_{12}$, the AC impedance spectroscopy of $\text{Li}_4\text{Ti}_5\text{O}_{12}$ -PAN and $\text{Li}_4\text{Ti}_5\text{O}_{12}$ at ambient temperature was conducted in the frequency range of 10^{-3} – 10^6 Hz as

shown in Fig.6. The open-circuit voltage is 1.52 V. A typical semicircle and an inclined line are seen in both curves of $\text{Li}_4\text{Ti}_5\text{O}_{12}$ -PAN and $\text{Li}_4\text{Ti}_5\text{O}_{12}$. The high frequency arc is attributed to the charge transfer reaction at the interface of electrolyte and electrode. The inclined line corresponds to Warburg impedance related to the diffusion of lithium ion in the anode.

The conductivity of the specimen is determined by the AC impedance spectroscopy at ambient temperature. According to the formula as follows[24]: $\sigma = d/AR$, where σ is the conductivity; R is the resistance; d is the diameter and A is the specific surface area. The conductivities of $\text{Li}_4\text{Ti}_5\text{O}_{12}$ -PAN and $\text{Li}_4\text{Ti}_5\text{O}_{12}$ are 8.6×10^{-7} S/cm and 4.4×10^{-7} S/cm, respectively. Since PAN does not enter the spinel structure, the PAN is just coated on the surface of $\text{Li}_4\text{Ti}_5\text{O}_{12}$ particle, and the increase of the conductivity in the PAN coated specimen is mainly due to the increase of the electronic conductivity of $\text{Li}_4\text{Ti}_5\text{O}_{12}$.

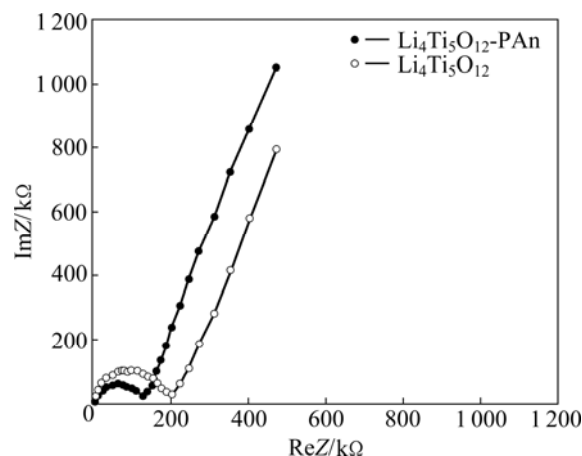


Fig.6 AC impedance plots of $\text{Li}_4\text{Ti}_5\text{O}_{12}$ -PAN and $\text{Li}_4\text{Ti}_5\text{O}_{12}$

4 Conclusions

1) $\text{Li}_4\text{Ti}_5\text{O}_{12}$ powders are prepared by so-gel method using tetrabutyl titanate, lithium acetate and absolute alcohol as starting materials. $\text{Li}_4\text{Ti}_5\text{O}_{12}$ -polyaniline ($\text{Li}_4\text{Ti}_5\text{O}_{12}$ -PAN) composite is prepared by in situ polymerization method using aniline, ammonium persulfate and hydrochloric acid as starting materials.

2) The electrical conductivity is enhanced obviously

Table 1 Comparison of cycling performance for $\text{Li}_4\text{Ti}_5\text{O}_{12}$ -PAN and $\text{Li}_4\text{Ti}_5\text{O}_{12}$ anode materials

Charge-discharge current rate	The 1st discharge capacity/(mA·h·g ⁻¹)		The 10th discharge capacity/(mA·h·g ⁻¹)		Capacity loss/%	
	$\text{Li}_4\text{Ti}_5\text{O}_{12}$ -PAN	$\text{Li}_4\text{Ti}_5\text{O}_{12}$	$\text{Li}_4\text{Ti}_5\text{O}_{12}$ -PAN	$\text{Li}_4\text{Ti}_5\text{O}_{12}$	$\text{Li}_4\text{Ti}_5\text{O}_{12}$ -PAN	$\text{Li}_4\text{Ti}_5\text{O}_{12}$
0.1C	191.3	195.2	177.0	179.4	0.75	0.81
0.2C	175.6	179.8	161.2	162.5	0.82	0.96
0.5C	164.5	168.5	149.5	149.3	0.91	1.14
1.0C	158.8	161.4	142.4	140.1	1.03	1.32
2.0C	148.9	149.3	131.6	125.9	1.16	1.57

due to the introduction of PAN to $\text{Li}_4\text{Ti}_5\text{O}_{12}$. $\text{Li}_4\text{Ti}_5\text{O}_{12}$ -PAN composite exhibits better high-rate capability and cyclability than $\text{Li}_4\text{Ti}_5\text{O}_{12}$. The composite can deliver a specific capacity of 191.3 and 148.9 mA·h/g, only 0.13% and 0.61% of the capacity is lose after being discharged 80 times at 0.1C and 2.0C, respectively.

References

- [1] FU L J, LIU H, WU Y P, RAHM E, HOLZE R WU H Q. Electrode materials for lithium secondary batteries prepared by sol-gel methods [J]. *Prog Mater Sci*, 2005, 50: 881–887.
- [2] WU Y P, DAI X B, MA J Q. Lithium ion batteries—Practice and application [M]. Beijing: Chemical Industry Press, 2004. (in Chinese)
- [3] AMATUCCI G, BADWAY F, PASQUIER A D, ZHENG T. An asymmetric hybrid nonaqueous energy storage cell [J]. *J Electrochem Soc*, 2001, 148(8): A930–939.
- [4] SINGHAL A, SKANDAN G, AMATUCCI G, BADWAY F, YEN MANTHIRAM A, YE H, XU J J. Nanostructured electrodes for next generation rechargeable electrochemical devices [J]. *J Power Sources*, 2004, 129(1): 38–44.
- [5] OHZUKU T, UEDA A, YAMAMOTO N. Zero-strain insertion material of $\text{Li}[\text{Li}_{1/3}\text{Ti}_{5/3}]\text{O}_4$ for rechargeable lithium cells [J]. *J Electrochem Soc*, 1995, 142(5): 1431–1435.
- [6] PROSINI P P, MANCINI R, PETRUCCI L, CONTINI V, VILIANO P. $\text{Li}_4\text{Ti}_5\text{O}_{12}$ as anode in all-solid-state, plastic, lithium-ion batteries for low-power applications [J]. *Solid State Ionics*, 2001, 144(1/2): 185–192.
- [7] KAVAN L, PROCHAZKA J, SPITLER T M, KALBA M, ZUKALOVA M, DREZEN T, GRATZEL M. Li insertion into $\text{Li}_4\text{Ti}_5\text{O}_{12}$ (Spinel) [J]. *J Electrochem Soc*, 2003, 150(7): A1000–1005.
- [8] HUANG S H, WEN Z Y, ZHU X J, GU Z H. Preparation and electrochemical performance of Ag doped $\text{Li}_4\text{Ti}_5\text{O}_{12}$ [J]. *Electrochem Commun*, 2004, 6(11): 1093–1097.
- [9] GUERFI A, CHAREST P A, KINOSHITA K, PERRIER M, ZAGHIBET K. Nano electronically conductive titanium-spinel as lithium ion storage negative electrode [J]. *Journal of Power Sources*, 2004, 126(1/2): 163–168.
- [10] GUERFI A, SE'VIGNY S, LAGACE' M, HOVINGTON P, KINOSHITA K, ZAGHIB K. Nano-particle $\text{Li}_4\text{Ti}_5\text{O}_{12}$ spinel as electrode for electrochemical generators [J]. *Journal of Power Sources*, 2003, 119/121: 88–94.
- [11] HE Ze-qiang, LIU Wen-ping, XIONG Li-zhi, CHEN Shang, WU Xian-ming, FAN Shao-bing. Preparation and electrochemical properties of $\text{Li}_4\text{Ti}_5\text{O}_{12}$ -C composite as anode for lithium ion batteries [J]. *Wujihuaxue Xuebao*, 2007, 23(4): 733–737. (in Chinese)
- [12] GUO Z P, WANG J Z, LIU H K, DOU S X. Study of silicon/polypyrrole composite as anode materials for Li-ion batteries [J]. *J Power Sources*, 2005, 146(1/2): 448–451.
- [13] DU PASQUIER A, ORSINI F, GOZDZ A S, TARASCON J M. Electrochemical behaviour of LiMn_2O_4 -PPy composite cathodes in the 4-V region [J]. *J Power Sources*, 1999, 81(1/2): 607–611.
- [14] VEERARAGHAVAN B, PAUL J, HALA B, POPOV B. Study of polypyrrole graphite composite as anode material for secondary lithium-ion batteries [J]. *J Power Sources*, 2002, 109(2): 377–387.
- [15] HE Ze-qiang, LIU Wen-ping, XIONG Li-zhi, SHU Hui, WU Xian-ming, CHEN Shang, HUANG Ke-long. Synthesis and characterization of SnO_2 -polyaniline composite as anode for lithium ion batteries [J]. *Wujihuaxue Xuebao*, 2007, 23(5): 813–826. (in Chinese)
- [16] POUGET J P, JOZEFOWICZ M E, EPSTEIN A J, TANG X, MACDIARMID A G. X-ray structure of polyaniline [J]. *Macromolecules*, 1991, 24(3): 779–789.
- [17] WU Yun, HU Li-li, JIANG Zhong-hong. Study on the electrochemical properties of Fe_2O_3 - TiO_2 films prepared by sol-gel process [J]. *J Electrochem Soc*, 1997, 144(5): 1728–1733.
- [18] PARK Y J, KIM J G, KIM M K, CHUNG H T, UM W S, KIM M H, KIM H G. Fabrication of LiMn_2O_4 thin films by sol-gel method for cathode materials of microbattery [J]. *J Power Sources*, 1998, 76(1): 41–47.
- [19] FUSALBA F, BELANGER D. Chemical synthesis and characterization of polyaniline-molybdenum trisulfide composite [J]. *J Mater Res*, 1999, 14(5): 1805–1813.
- [20] WANGM X. Absorption spectra of thin film of polyaniline [J]. *J Polymer Science Part A: Polymer Chemistry*, 1992, 30(4): 543–549.
- [21] HAO Yan-jing, LAI Qiong-yu, XU Zhi-hui, LIU Xue-qi, JI Xiao-yang. Synthesis by TEA sol-gel method and electrochemical properties of $\text{Li}_4\text{Ti}_5\text{O}_{12}$ anode material for lithium-ion battery [J]. *Solid State Ionics*, 2005, 176(13/14): 1201–1206.
- [22] NAKAHARA K, NAKAJIMA R, MATSUSHIMA T, MAJIMA H. Preparation of particulate $\text{Li}_4\text{Ti}_5\text{O}_{12}$ having excellent characteristics as an electrode active material for power storage cells [J]. *J Power Sources*, 2003, 117(1/2): 131–136.
- [23] HUANG S H, WEN Z Y, ZHANG J C, GU Z H, XU X H. $\text{Li}_4\text{Ti}_5\text{O}_{12}$ /Ag composite as electrode materials for lithium-ion battery [J]. *Solid State Ionics*, 2006, 177: 851–855.
- [24] ROBERTSON A D, TUKAMOTO H, IRVINE J T S. $\text{Li}_{1-x}\text{Fe}_{1-3x}\text{Ti}_{1+2x}\text{O}_4$ ($0 < x < 0.33$) based spinels: Possible negative electrode materials for future Li-ion batteries [J]. *J Electrochem Soc*, 1999, 146(11): 3958–3962.
- [25] SCHARNER S, WEPPNER W, SCHMID-BEURMANN P. Evidence of two-phase formation upon lithium insertion into the $\text{Li}_{1.33}\text{Ti}_{1.67}\text{O}_4$ spinel [J]. *J Electrochem Soc*, 1999, 146(3): 857–861.

(Edited by ZHAO Jun)